Clinical Case Report

Medicine®

OPEN

Multimodality imaging features, treatment, and prognosis of post-transplant lymphoproliferative disorder in renal allografts

A case report and literature review

Jianming Li, MD[a], Yujiang Liu, MD[a], Zhenchang Wang, MD[b], Xiangdong Hu, MD[a], Ruifang Xu, MD[a], Linxue Qian, MD[a,*]

Abstract

Rationale: Among patients with post-transplant lymphoproliferative disorder (PTLD), there is a high incidence of immunosuppressed transplant recipients. It is necessary to make an early diagnosis to increase the likelihood of a good prognosis.

Patient concerns: We report a case of a 54-year-old female patient who developed PTLD after liver and kidney transplantation.

Diagnoses: We aimed to analyze the standard diagnosis and follow-up of PTLD with imaging. Radiologists need to be familiar with all imaging modalities when dealing with PTLD, including ultrasonography, computed tomography, magnetic resonance imaging, positron-emission tomography/computed tomography.

Interventions: The initial treatment included both reduction of immunosuppression and rituximab. Then the treatment strategy changed to rituximab and chemotherapy. Finally, the treatment strategy combined glucocorticoid therapy.

Outcomes: The patient was in a stable condition at the 3-month follow-up.

Lessons: Systematic evaluation of the various imaging modalities, treatment options, and prognoses of PTLD in renal allografts suggested that in cases with a poor prognosis, the proper imaging modalities provide essential information with regard to the determination of the appropriate treatment.

Abbreviations: ADC = apparent diffusion coefficient, CDUS = color Doppler ultrasonography, CECT = contrast-enhanced computed tomography, CE-MRI = contrast-enhanced magnetic resonance imaging, CEUS = contrast-enhanced ultrasonography, CMV = cytomegalovirus, CPR = curve planar reformation, CT = computed tomography, DWI = diffusion-weighted imaging, EBV = Epstein–Barr virus, FDG = fluorodeoxyglucose, MRI = magnetic resonance imaging, PET/CT = positron-emission tomography/computed tomography, PTLD = post-transplant lymphoproliferative disorder, RIS = reduction in immunosuppression, SUV = standard uptake value, T1WI = T1-weighted imaging, T2WI = T2-weighted imaging, US = ultrasonography.

Keywords: diagnosis, multimodality imaging, prognosis, PTLD, renal transplantation

1. Introduction

Renal transplantation is the preferred treatment in end-stage renal disease, both in terms of quality of life and long-term survival. However, due to the postoperative requirement for immunosuppression, the risks of Epstein–Barr virus (EBV) and cytomegalovirus (CMV) infection are increased. These viruses are risk factors for post-transplant lymphoproliferative disorder (PTLD). PTLD represents abnormal lymphoid proliferation ranging from polyclonal lymphoid proliferation to malignant lymphomas.[1,2] Prompt diagnosis of PTLD is critical to prognosis, to prevent the further development of malignant lymphoma.[3] A variety of imaging methods serve different purposes in the diagnosis of PTLD, including ultrasonography (US), contrast-enhanced US (CEUS),[4] computed tomography (CT), magnetic resonance imaging (MRI), contrast-enhanced MRI (CE-MRI),[5] and positron-emission tomography/CT (PET/CT).[6]

2. Case report

This study was approved by the institutional review board at the Beijing Friendship Hospital of Capital Medical University, and informed consent was obtained from the patient.

2.1. Medical history

The subject was a 54-year-old female patient with polycystic liver and kidney disease for > 10 years. Her mother also had this disease. She suffered from hypertension for 20 years (the highest blood pressure: 200/100 mm Hg). She had been on antihypertensive treatment (nifedipine: 10 mg) for 4 years. Because of severe renal

Editor: N/A.

All authors: Beijing Friendship Hospital.

The authors report no conflicts of interest.

[a] Department of Ultrasound, [b] Department of Radiology, Capital Medical University, Beijing, China.

[*] Correspondence: Linxue Qian, Department of Ultrasound, Beijing Friendship Hospital, Capital Medical University, No. 95 Yong'an Road, Xicheng District, Beijing 100050, China (e-mail: Qianlinxue2002@163.com).

Medicine (2018) 97:17(e0531)

Received: 31 December 2017 / Received in final form: 29 March 2018 / Accepted: 2 April 2018

http://dx.doi.org/10.1097/MD.0000000000010531

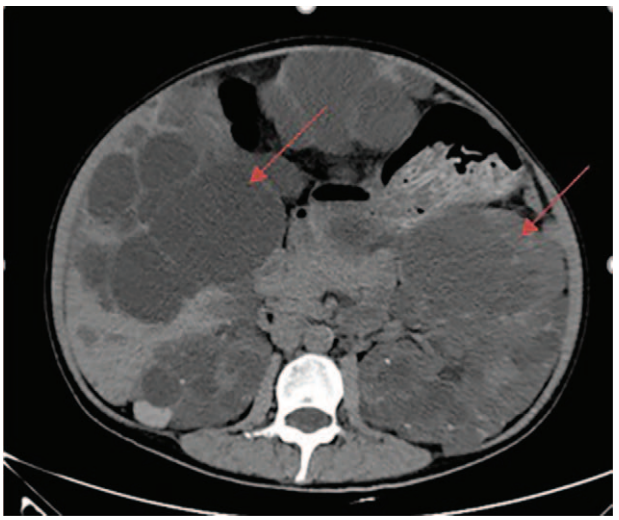

Figure 1. Preoperative. A 54-year-old female patient with polycystic liver and kidney disease.

insufficiency, the patient received liver and kidney transplantation for polycystic liver and kidney disease (Fig. 1) 1 month post-surgery. The disease history is summarized in Table 1.

2.2. Physical examination

The patient had obvious abdominal distension, and abdomen was nontender and bowel sounds were fine. The patient had a regular pulse of 70 beats/min, a respiratory rate of 20 breaths/min, and a temperature of 36.8°C, a blood pressure of 140/90 mm Hg. No icterus was apparent and superficial lymph nodes were not palpable. Cardiovascular and neurologic examinations were normal.

2.3. Laboratory results

The patient had severe renal insufficiency (serum creatinine: 367 μmol/L) and renal anemia (white blood cell count: 7.11×10^9/L, red blood cell count: 3.92×10^{11}/L, hemoglobin level: 119.0 g/L, platelet count: 142×10^9/L) before the operation. The patient was poor physical condition postsurgery, which included liver dysfunction (alanine aminotransferase [ALT] 130 U/L, glutamic oxalacetic transaminase (AST) 150.8 U/L, gamma-glutamyltransferase (GGT) 93 U/L) and hematuresis. Two months later, the patient experienced a complicated urinary tract infection (creatinine: 379.4 μmol/L).

Table 1

Patient disease history.

Disease history	Description
Polycystic liver	>10 y before the surgery
Polycystic kidney	>10 y before the surgery
Renal insufficiency	2 y before o the surgery
Hypertension	20 y before the surgery
Liver dysfunction	3 mo postsurgery
Hematuresis	3 mo postsurgery
Urinary tract infection	5 mo postsurgery
Graft rejection reaction	3 mo postsurgery
Family history	Yes
Other diseases	No

2.4. Imaging examination

One month after surgery, routine postoperative CT did not reveal any abnormalities (Fig. 2). However, after 2.5 months, US detected 1 clearly hypoechoic solid mass at the renal hilum, measuring approximately $1.6 \times 1.9 \times 1.4$ cm (Fig. 3). Four months later, MRI revealed 2 masses, one located in the renal allograft sinus (approximately 1.6×1.3 cm) and the other located in the renal pelvis (approximately 1.4×1.1 cm) (Fig. 4). Two months later, the renal allograft sinus and pelvic masses had increased to 1.7×2.2 and 1.5×1.8 cm, respectively. They were slightly hypointense on T1-weighted imaging (T1WI) and T2-weighted imaging (T2WI). They were also hyperintense on diffusion-weighted imaging (DWI), with low values on apparent diffusion coefficient (ADC) mapping. The main enhancement pattern of the renal masses manifested as gradual enhancement from the periphery to the center (Fig. 5).

Grayscale US demonstrated 2 clearly hypoechoic solid masses measuring approximately $1.7 \times 1.5 \times 1.7$ and $2.1 \times 1.9 \times 1.5$ cm. Color Doppler US (CDUS) suggested that the masses were not invading the peripheral vessels, but expanding extrinsically in the renal sinus and pelvis (Fig. 6). In CEUS with a 2.4-mL bolus of SonoVue (Bracco, Italy), the masses exhibited heterogeneous echogenicity and early peripheral enhancement in the cortical phase. Enhancement had progressed 15 seconds post-injection of SonoVue, sparing the center of each lesion. During the parenchymal phase, the masses gradually became hypoechoic compared with the renal cortex. The peripheral enhancement with central nonenhancement observed suggested central necrosis (Fig. 7).

2.5. Pathology

Under US guidance, core needle biopsy of the renal masses was performed (Fig. 8). Final pathology of the biopsy specimen confirmed PTLD, specifically malignant pleomorphic lymphoma (Fig. 9), and Epstein–Barr virus (EBV) positivity (Fig. 10). The serum was positive for EBV DNA in a quantitative test.

2.6. Therapeutic intervention and outcomes

Given the patient's poor physical condition postsurgery, which included liver dysfunction and hematuresis, we administered antirejection therapy (Medrol 8 mg/qd; FK506 1 mg/q 12 h; 46 days) and observed the masses over time via regular examinations (2–3 months). Two months later, the patient experienced a complicated urinary tract infection accompanied by frequent urination, pelvic pain, and elevated creatinine (379.4 μmol/L).

The initial treatment included both reduction of immunosuppression and rituximab. However, the patient experienced liver dysfunction again (ALT 130 U/L, AST 150.8 U/L, GGT 93 U/L), so immunosuppression was immediately increased (Medrol 4 mg/qd; FK506 0.25 mg/q 12 h; 20 days) for liver protection. Owing to the continuous enlargement of PTLD, it fused and increased to $4.9 \times 5.0 \times 4.3$ cm, involving the entire ureter after 9 months (Figs. 11 and 12). Transplantation doctors changed the treatment strategy to rituximab (600 mg; 1 day) and chemotherapy (cyclophosphamide 600 mg/dL; vincristine 2 mg/dL; prednisone, 10 mg/dL; 4 days). In case of graft rejection, transplantation doctors combined glucocorticoid therapy (20 mg/q 12 h; 5 days). The patient was in a stable condition at the 3-month follow-up.

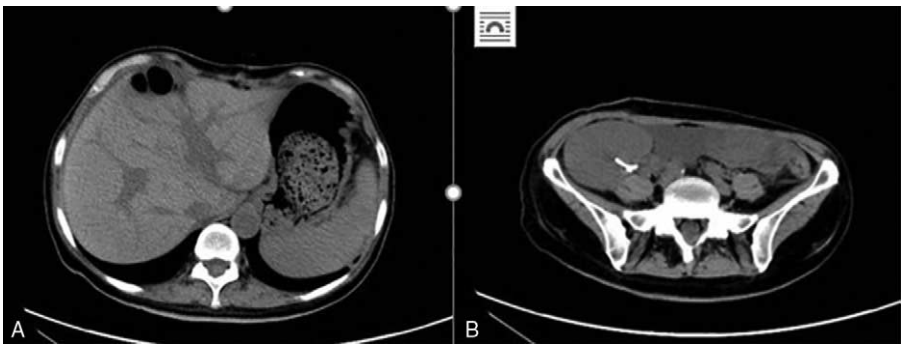

Figure 2. Postoperative. One month after liver and kidney transplantation, computed tomography of the liver (A) and kidney allografts (B) do not reveal any abnormal densities. CT = computed tomography.

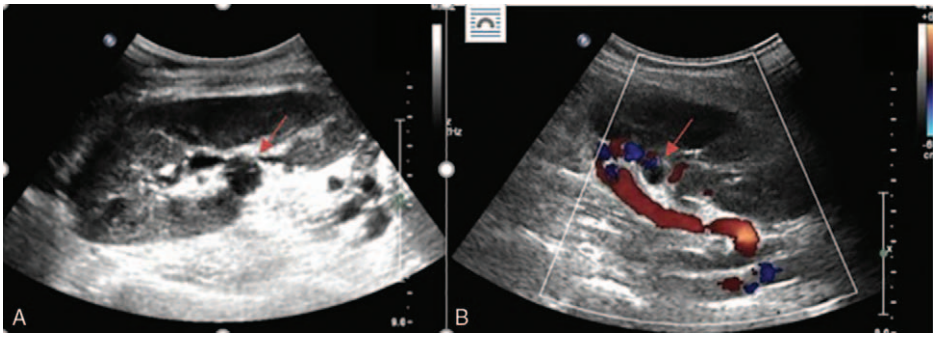

Figure 3. Ultrasonography (A) and color Doppler ultrasonography (B) images initially depicted 1 hypoechoic mass located in the hilum. CDUS = color Doppler ultrasonography, US = ultrasonography.

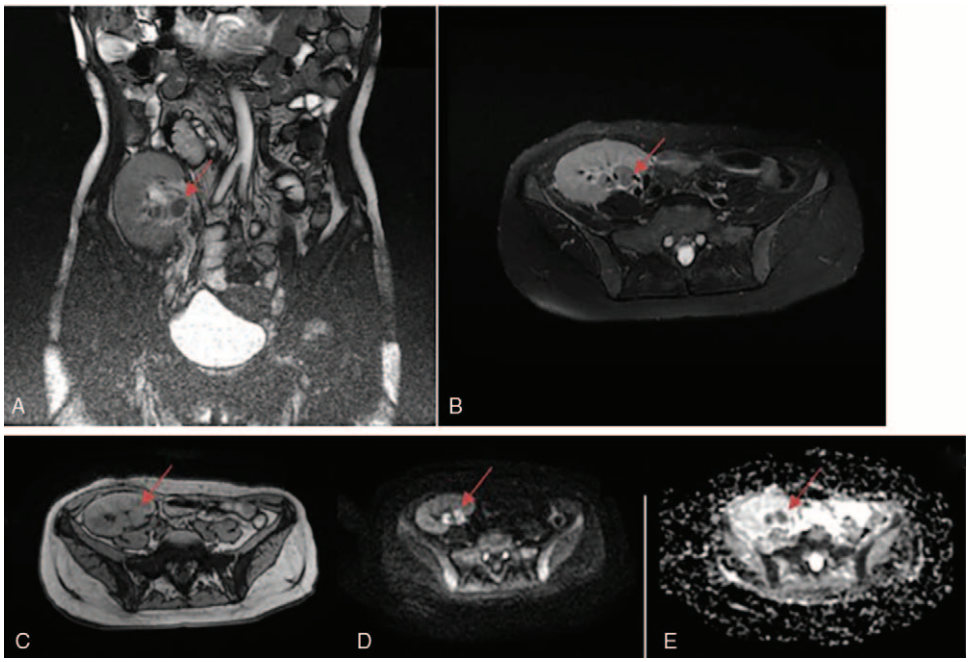

Figure 4. Magnetic resonance imaging depicted 2 abnormal emerging tumor-like masses in the transplant's renal medulla. The coronal (A)/axial (B) position of a T2-weighted imaging sequence revealed emerging masses with slight hypointensity. The axial position of a T1-weighted imaging sequence (C) also depicted emerging masses with slight hypointensity. The diffusion-weighted imaging sequence (D) depicted obvious hyperintensity with decreased apparent diffusion coefficient values (E). ADC = apparent diffusion coefficient, DWI = diffusion-weighted imaging, MRI = magnetic resonance imaging, T1WI = T1-weighted imaging, T2WI = T2-weighted imaging.

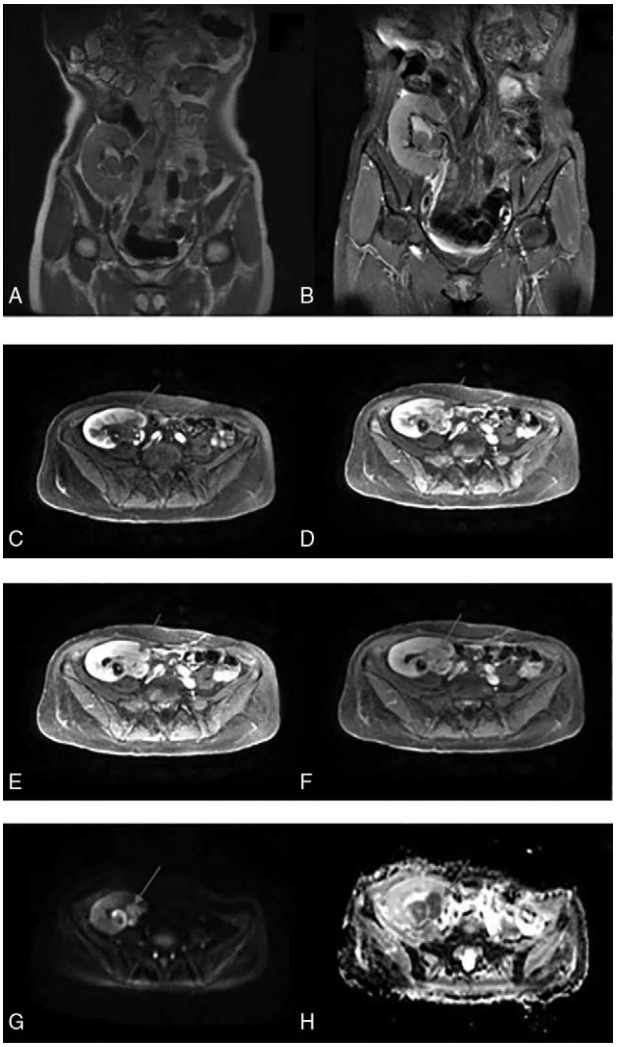

Figure 5. Repeated examination 2 months later. T2-weighted imaging (A)/T2-weighted imaging + fat suppression (B) sequence depicted persistent slight hypointensity, but the lesions were bigger. Dynamic contrast enhancement scanning (C–F) showed persistent peripheral enhancement. The diffusion-weighted imaging sequence (G) and apparent diffusion coefficient value (H) were similar to those of the previous examination. ADC = apparent diffusion coefficient, DWI = diffusion-weighted imaging, T2WI = T2-weighted imaging.

Imaging examinations and treatment procedures are described in Fig. 13.

3. Discussion

The clinical features of PTLD are usually nonspecific. Patients may exhibit unclear symptoms such as allograft dysfunction, fever, or abdominal pain.[2] Modern imaging is an essential tool in early diagnosis and staging of lesions. However, there are few systematic reviews about each imaging modality's features, advantages, and associations with treatment and prognosis of PTLD following renal transplantation, due to lack of concrete analysis.

3.1. Etiology

Immunosuppression is necessary for post-transplant patients. In a state of immunosuppression and in settings with a high incidence of EBV infection, patients are at risk of the development of malignant monoclonal lymphoma.[2] PTLD occurred in approximately 1% of renal allograft recipients in the year 2000,[7] and developed in approximately 3% of patients following renal transplantation in the year 2017.[3] PTLD exhibits a "U-shaped" pattern of incidence in conjunction with transplantation time, so it is subdivided into early-onset and late-onset subtypes.[8] The 2 subtypes exhibit different biological characteristics. Early-onset PTLD tends to occur in younger patients who are EBV or CMV positive, and tumors in this population have a higher incidence of location within the transplanted organ.[8] The current patient was EBV positive and the masses had increased in size 4 months postoperatively, suggesting that this case was early-onset PTLD, although her age was uncharacteristic. Late-onset PTLD involves a higher proportion of older patients and is often of T-cell origin.[8] Therefore, clinicians should be familiar with the relevant epidemiological features, anticipating the bimodal distribution.

3.2. Clinical and imaging diagnosis

PTLD is divided into 2 major categories based on its primary location: nodal and extranodal. Because the current case was located in a renal allograft, we mainly considered various extranodal PTLD imaging patterns secondary to renal transplantation. Solid organ PTLD can be divided into 4 imaging patterns, obstructive, solitary mass, parenchymal (scattered), and

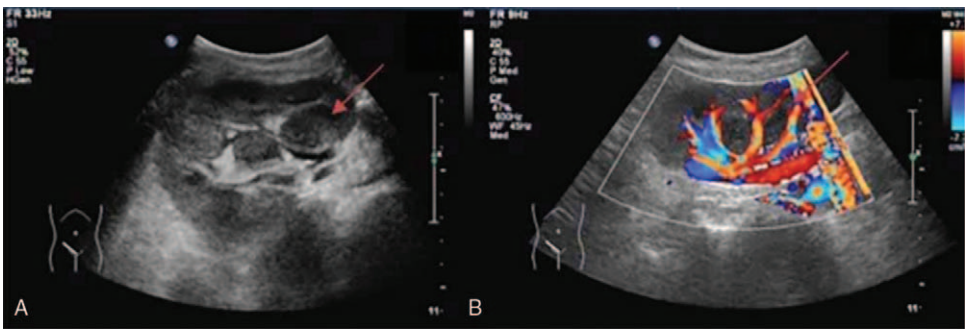

Figure 6. Ultrasonography (A) and color Doppler ultrasound (B) depicted 2 hypoechoic masses located in the hilum, with no evidence of infiltration or an effect on surrounding blood vessels. CDUS = color Doppler ultrasound, US = ultrasonography.

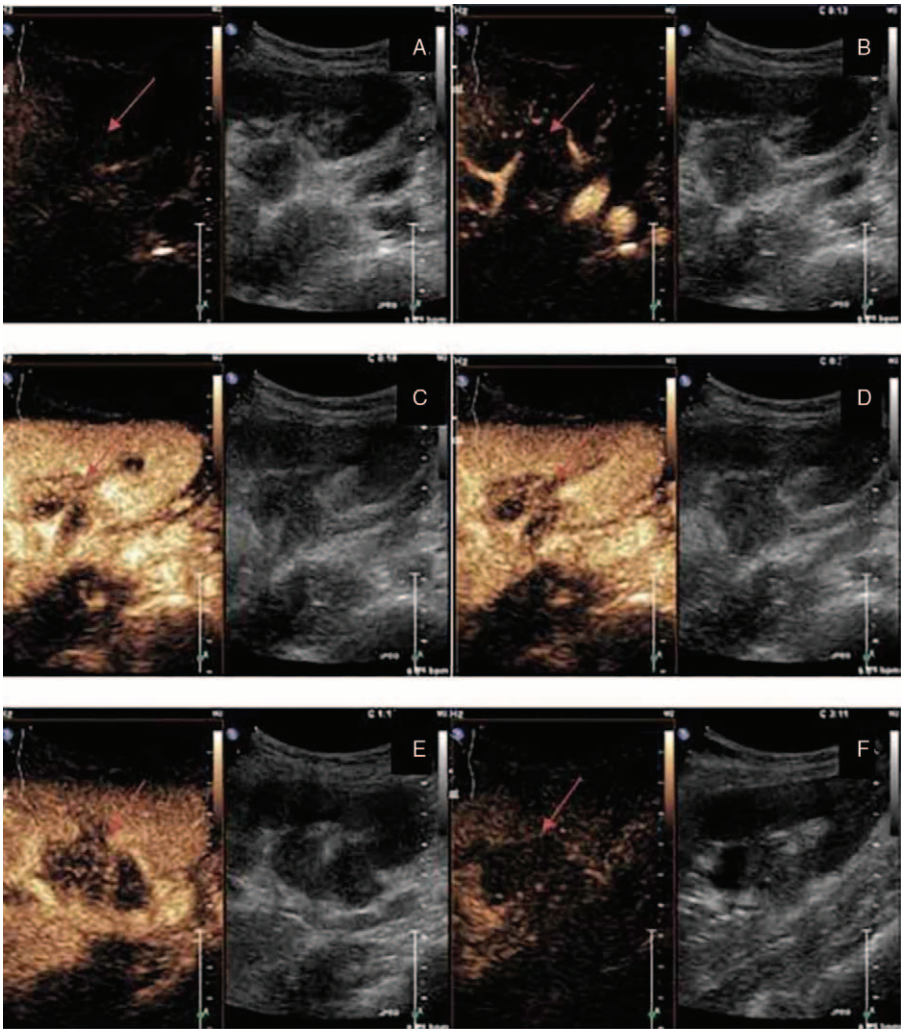

Figure 7. A series of contrast-enhanced ultrasonography (CEUS) images. (A) The initial image from the start of CEUS (0 s after injection) showed hypoechoic renal cortex, medulla, and mass, and bright background echoes in the perinephric and renal sinus fat. (B) Imaging from the cortical enhanced phase (13–20 s after injection) depicted hypoenhancing mass at 13 s. (C) Two obviously heterogeneous enhancing masses were evident in the image at 18 s. (D) Nephrographic phase (30 s after injection) CEUS imaging depicted initial decrease in enhancement in the mass, earlier than in the cortex. (E) Imaging depicted hypoenhancement in the mass against the enhanced background of the renal cortex. (F) End of CEUS examination image at 3 min shows washout of enhancement of the renal cortex, medulla, and mass. Throughout the CEUS examination, all images of the masses showed progressive peripheral enhancement with central nonenhancement. CEUS = contrast-enhanced ultrasonography.

infiltrative.[2] When the kidney is affected, the primary imaging pattern is the obstructive pattern. A mass located outside the renal hilum can result in extrinsic compression or obstruction of the nonvascular outflow of the kidney, causing blood vessel obstruction and renal collecting system obstruction.[2] As the PTLD progresses, the infiltrative pattern depicts a lesion that extends from the affected organ and involves surrounding structures or adjacent organs.[2] Adrenal involvement is relatively less common, and other infiltrative appearances include the manifestation of diffuse lesions with renal enlargement.[9] In the current case, the PTLD involved the entire ureter.

3.3. CT

The anatomic details of the graft and associated lesions could be clearly visualized via CT and MRI. When the patient was asymptomatic, CT findings of PTLD were nonspecific and difficult to interpret. The most common appearance is a solitary, round, solid, low-density mass involving a normal-sized graft.[9] An atypical CT sign of PTLD is a diffusely infiltrating process causing renal enlargement.[9] The renal hilum anastomosis is the most common site for renal PTLD development, and the lesion frequently encases the hilar vessel.[10] Involvement of other organs and vessels is less common, and calcifications may be present.[10] If the patient has favorable kidney function, the hilar mass shows mild enhancement upon the administration of contrast material.[7] Due to the risk of nephrotoxicity from the contrast materials, contrast-enhanced computed tomography (CECT) is usually avoided.[11] We did not make an early diagnosis via CT alone until severe infection and abnormal function of the renal allograft occurred.

3.4. MRI

Due to its superior contrast resolution, multiplanar capability, lack of ionizing radiation, and lack of operator dependence, Ali

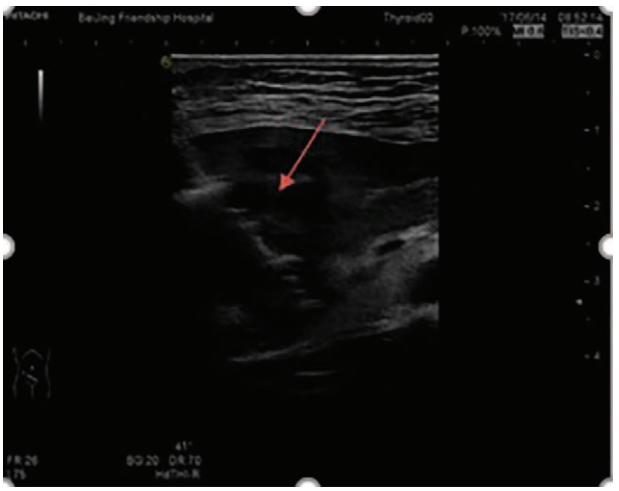

Figure 8. Ultrasonography with core biopsy needle in the hypoechoic mass at the hilum of the transplanted kidney. US = ultrasonography.

et al[12] recommended MRI over US or CT in the evaluation of post-transplantation renal allograft abnormalities. The common signal intensity and enhancement characteristics of PTLD were determined to be hypointensity on T1WI and T2WI with minimal or mostly peripheral enhancement on postcontrast images.[12] There was a homogeneous hypointense pattern of diffusivity on the ADC maps, and a hyperintense pattern on DWI (Fig. 4), in which there was relatively restricted diffusion at lesions corresponding to the dense cellular infiltrates. This is the same signal pattern seen in central nervous system PTLD, as described by Ginat et al.[5] The mass may encase vessels at the renal hilum. As with CECT examination, attention should be paid to nephrogenic systemic damage,[11] and CE-MRI with gadolinium also requires considered application.

3.5. US/CEUS

US/CDUS has the advantage of nontoxic contrast, repeatability, and an ability to provide physiologic information about the allograft. US has historically been the first-line and primary screening modality for renal allografts. However, it can be difficult to identify small ill-defined PTLD masses via US. Lopez-Ben et al[7] confirmed that complex hypoechoic masses adjacent to the renal hilum are the usual initial US findings. Because the masses can compress the ureter, hydronephrosis was always observed in the authors' experience, but CT or MRI was superior for the detection of the disease. Thus, US and CDUS have similar limitations with regard to the assessment of PTLD masses.

CEUS relies on intravenous injection of encapsulated microbubbles of gas with coating materials that are primarily metabolized by the liver. When compared with CECT and CE-MRI, CEUS has favorable imaging advantages in renal transplant recipients because it is non-nephrotoxic (thus, nephrologists prefer to use it).[4] CEUS has much higher sensitivity and specificity for the detection of complications of renal transplants, providing quantitative information on microvascular perfusion

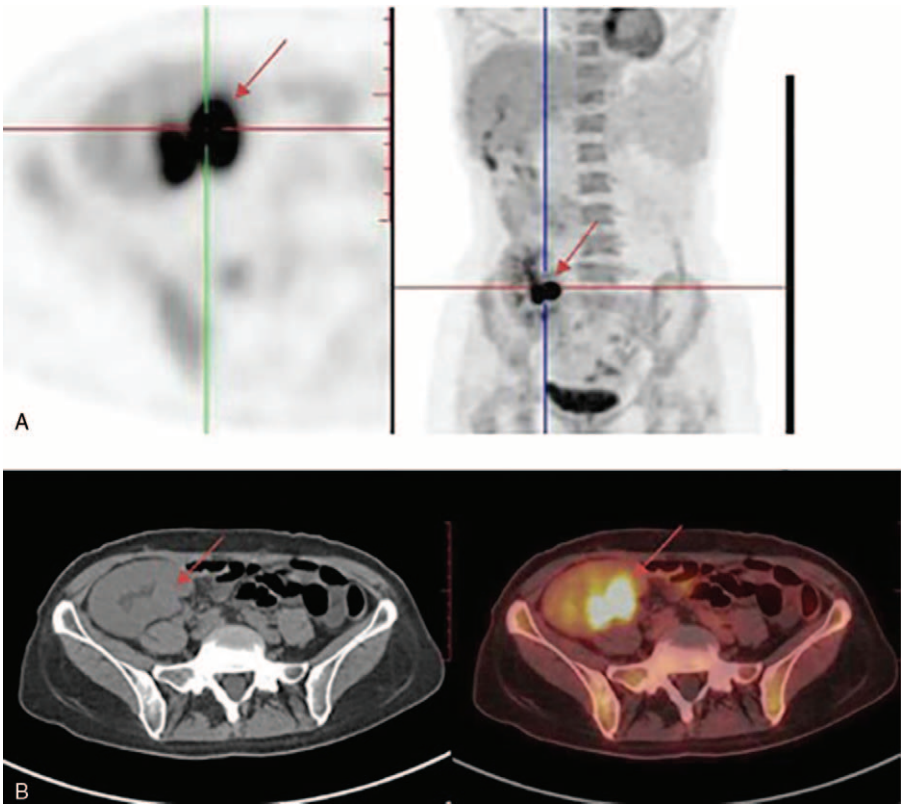

Figure 9. Hematoxylin and eosin staining of the core needle biopsy specimen from the mass revealed lymphocytic infiltration. (A) × 100, (B) × 200.

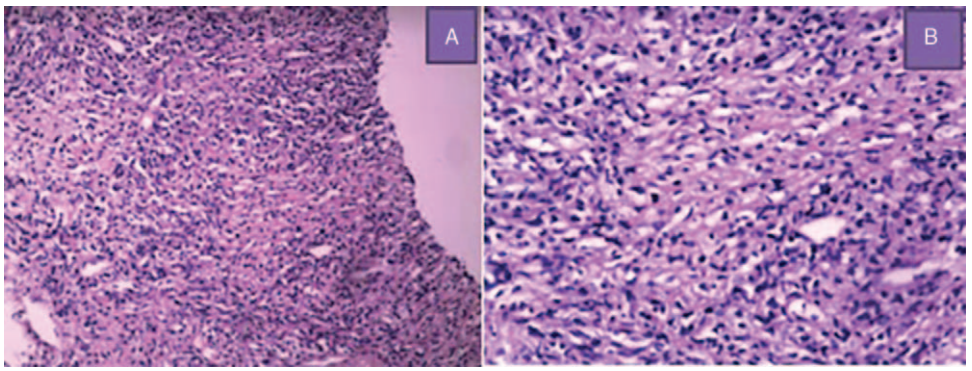

Figure 10. The lymphocytes exhibited positivity for Epstein–Barr virus-encoded RNA in an in situ hybridization stain (×100). EBV = Epstein–Barr virus.

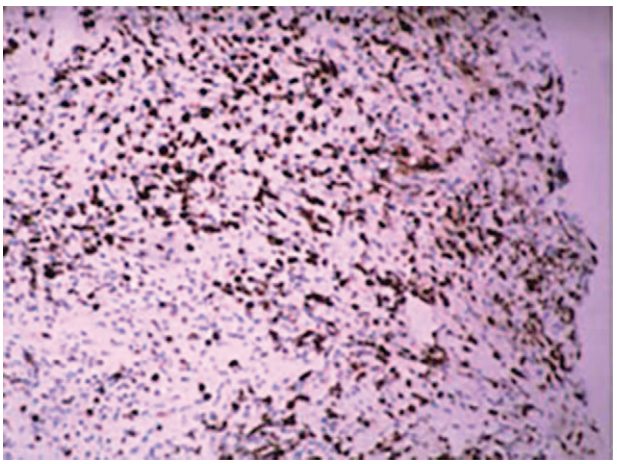

Figure 11. Nine months after post-transplant lymphoproliferative disorder (PTLD) was first detected, ultrasonography (A, B, C, E) and color Doppler ultrasonography (D, F) images demonstrated that PTLD was enlarged and involved the entire ureter. Abundant blood flow signals in the ureter were apparent in color Doppler ultrasonography imaging. CDUS = color Doppler ultrasonography, PTLD = post-transplant lymphoproliferative disorder, US = ultrasonography.

of the renal allografts and the diagnosis of chronic allograft nephropathy.[13] Due to the predilection of PTLD to encase the hilar vessels, diagnosing PTLD via core needle biopsy is risky.[12] In the current case, we successfully obtained tissue via transcortical biopsy by carefully identifying the needle path (Fig. 8).

3.6. PET-CT

It has been proposed that PET-CT is an accurate diagnostic tool for assessing the disease extent and stage in PTLD patients, and the follow-up treatment response of PTLD (Figs. 14 and 15).[6] Noraini et al[14] suggest further study of the possible relationships between PET-CT findings and PTLD subtypes. The major advantage of PET-CT is high sensitivity with regard to the detection of normal-sized lesions with tumor involvement. PET-CT mainly uses fluorodeoxyglucose (FDG), avoiding contrast-related nephrotoxicity. When the kidney is affected by PTLD, PET-CT depicts increased FDG uptake, and the level of FDG uptake correlates with tumor grade.[2] In addition, the standard uptake value (SUV) calculation can provide a predictive value relating to patient prognosis. Higher SUV_{max} values indicate more severe disease activity.[14] However, PET-CT is inevitably

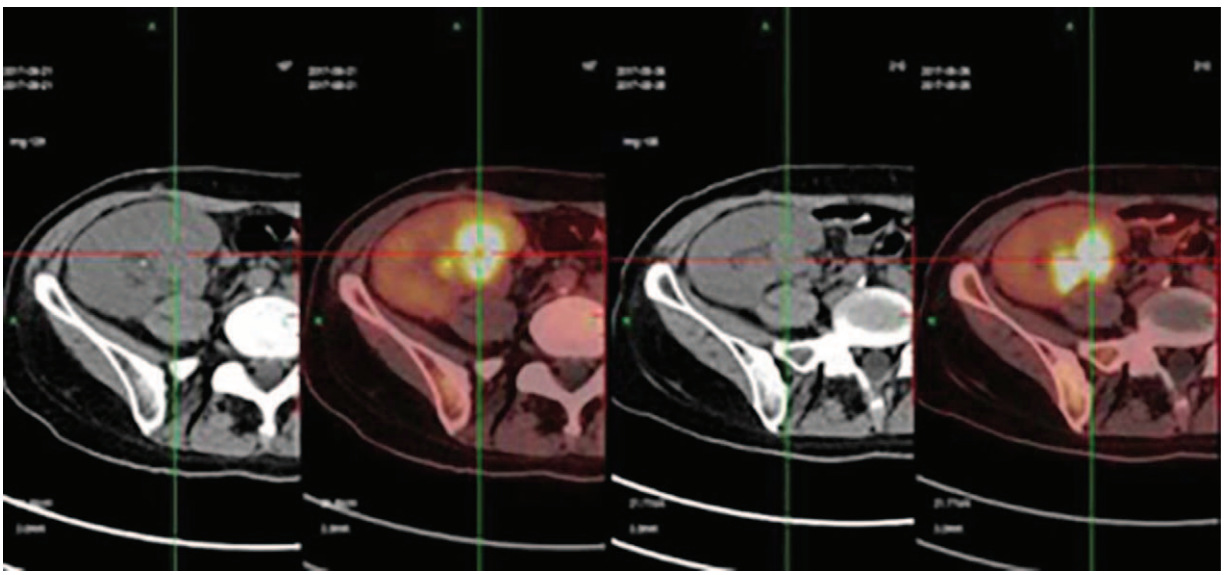

Figure 12. Computed tomography images taken in the axial position (A, B), coronal position (C), and curve planar reformation (D) showed enlargement of the tumor and ureter. CPR = curve planar reformation, CT = computed tomography.

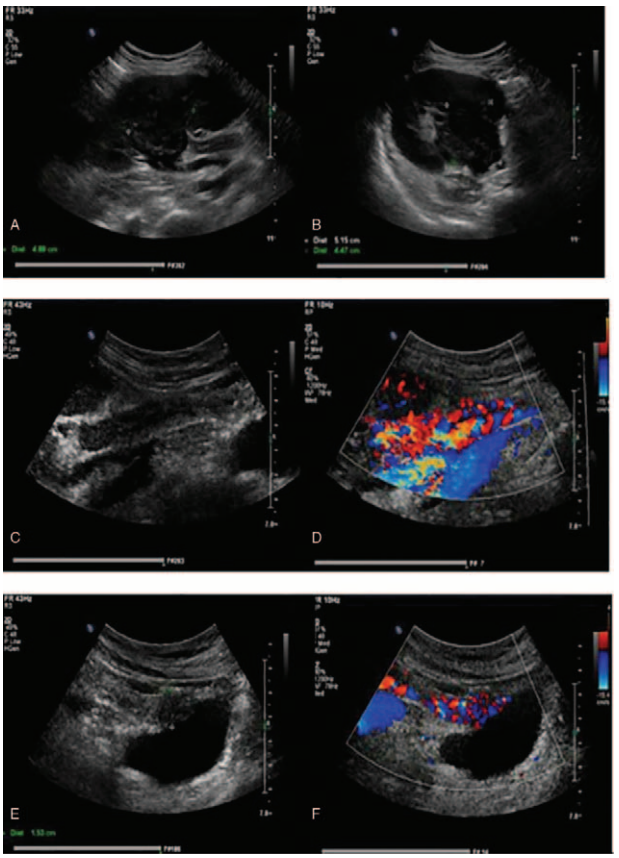

Figure 13. Imaging examinations and treatment procedures are described in timeline.

associated with a higher radiation dose and inferior specificity for differential diagnosis of diseases (higher false-positive rates) than US, CT, and MRI, and it is costly.

In the current case, the patient was examined via MRI, and we detected 2 masses with slight hypointensity on T1WI and T2WI and obvious hyperintensity on DWI. The lesions grew larger over the ensuing 2 months. The pattern of contrast enhancement suggested that peripheral enhancement was related to the central region. Similar to the MRI appearance, grayscale US and CDUS depicted 2 hypoechoic noninfiltrative masses located in the hilum with no effect on surrounding blood vessels. CEUS depicted peripheral enhancement with central nonenhancement.

3.7. Treatment and prognosis

Several risk factors, including infection, duration of immunosuppression, age, race, and genetic factors, can increase the risk of PTLD. In organ transplant patients with PTLD in remission, there is a conundrum in that immunosuppression is required for graft protection, but increases the risk of lymphoma progress. The management of PTLD is a complex task, with different treatment options, including reduction in immunosuppression (RIS), chemotherapy, rituximab, radiotherapy, antiviral agents with arginine butyrate, and surgery.[15] Patients who suffer from EBV-positive PTLD, early lesions, or polyclonal PTLD usually have a favorable response to RIS. Chemotherapy is a common

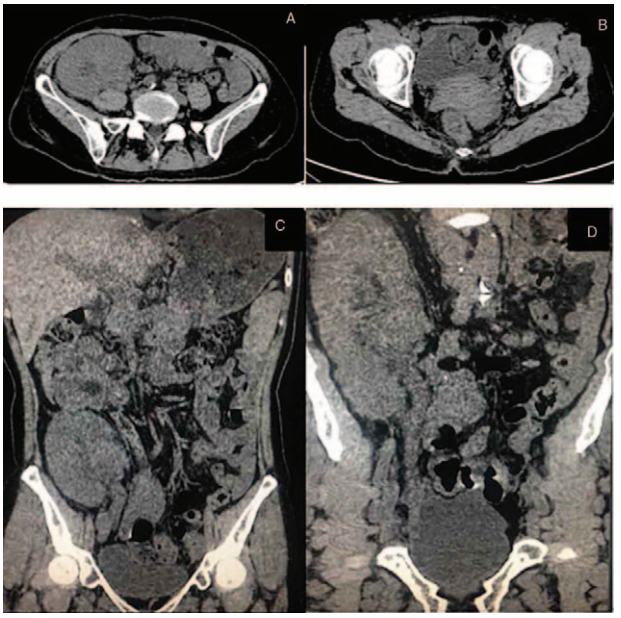

Figure 14. Images from positron-emission tomography/computed tomography revealed 2 masses of abnormal metabolic activity with intense fluorodeoxyglucose uptake. (A) Positron-emission tomography. (B) Computed tomography, left; fused, right. FDG = fluorodeoxyglucose, PET/CT = positron-emission tomography/computed tomography.

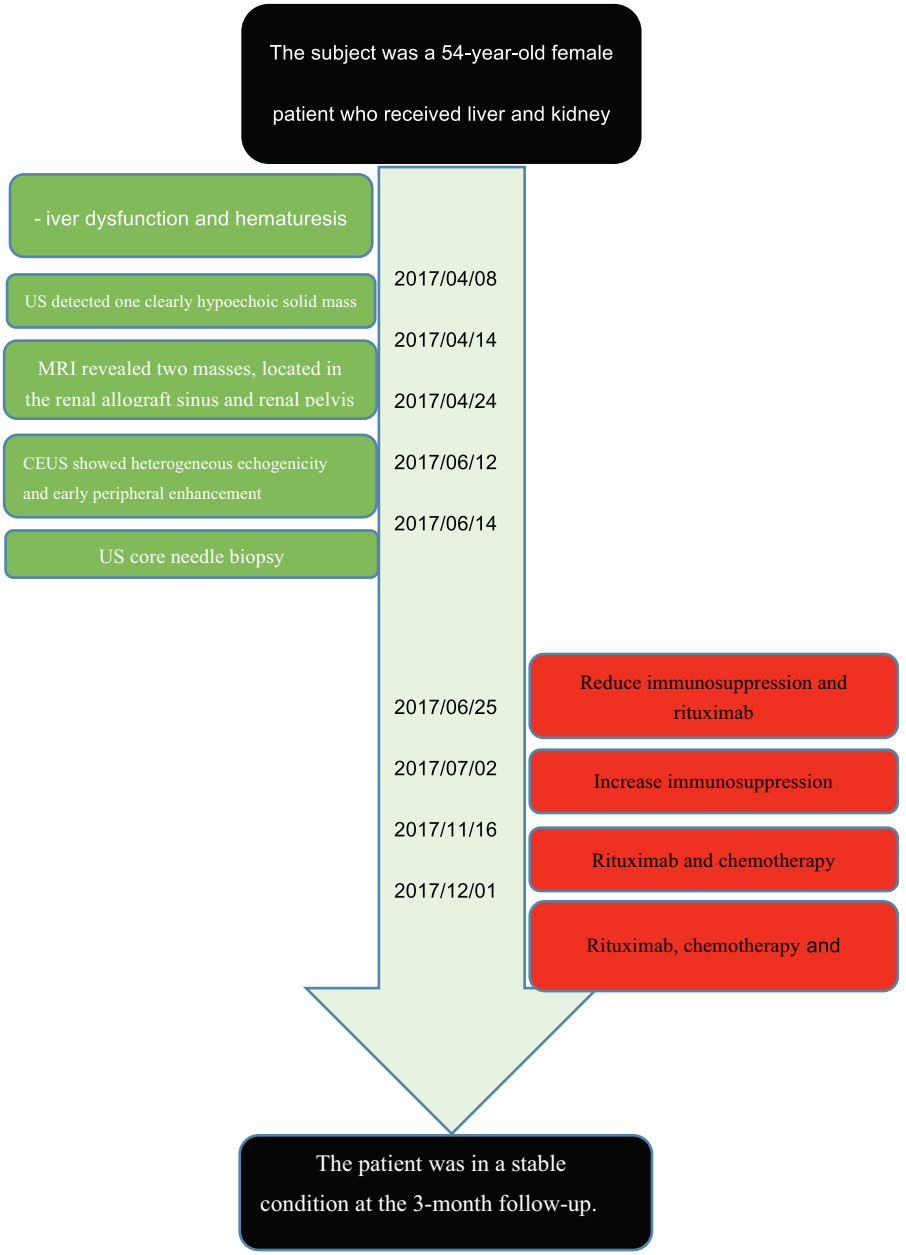

Figure 15. In a positron-emission tomography/computed tomography scan performed 3 months after the previous one, there were no obvious changes in post-transplant lymphoproliferative disorder. PET/CT = positron-emission tomography/computed tomography, PTLD = post-transplant lymphoproliferative disorder.

method when RIS fails, but may be accompanied by toxic complications. Rituximab is a breakthrough treatment and the first-line treatment option for PTLD. Although there is a high risk of PTLD recurrence, rituximab combined with chemotherapy is appropriate for poor-prognosis and high-risk groups.[16] If the PTLD was treated with RIS and chemotherapy, rituximab can effectively compensate for the negative impact of RIS.[17] Surgical resection and radiotherapy are suitable for localized PTLD or local complications of PTLD. Saadat et al[18] recommend decreasing or withdrawing immunosuppression, especially cyclosporine, which helps to increase tumor regression. The prognosis of early PTLD is now better, and with appropriate treatment, 30% of patients exceed 5-year survival.[15]

4. Conclusion

To the best of our knowledge, few systematic assessments of the various imaging modalities, treatment options, and prognosis considerations pertaining to PTLD have been previously reported. The role of medical imaging is crucial because early diagnosis of PTLD increases the chances of tumor regression through treatment. Consequently, by combining appropriate imaging examinations and clinical treatment, the standard management of PTLD will result in a better prognosis.

Author contributions

Conceptualization: linxue Qian.

Data curation: Jianming Li, Yujiang Liu.
Formal analysis: Jianming Li.
Methodology: Jianming Li, Yujiang Liu, Xiangdong Hu.
Project administration: linxue Qian.
Supervision: Zhenchang Wang.
Validation: Ruifang Xu.
Writing – original draft: Jianming Li.
Writing – review & editing: Jianming Li, Zhenchang Wang.

References

[1] Sabattini E, Bacci F, Sagramoso C, et al. WHO classification of tumours of haematopoietic and lymphoid tissues in 2008: an overview. Pathologica 2010;102:83–7.
[2] Camacho JC, Moreno CC, Harri PA, et al. Posttransplantation lymphoproliferative disease: proposed imaging classification. Radiographics 2014;34:2025–38.
[3] Abu-Shanab A, Ged Y, Ullah N, et al. Increased incidence of post-transplant lymphoproliferative disorder in autoimmune liver disease: an Irish national experience. J Clin Exp Hepatol 2017;465:8.
[4] Sanchez K, Barr RG. Contrast-enhanced ultrasound detection and treatment guidance in a renal transplant patient with renal cell carcinoma. Ultrasound Q 2009;25:171–3.
[5] Ginat DT, Purakal A, Pytel P. Susceptibility-weighted imaging and diffusion-weighted imaging findings in central nervous system monomorphic B cell post-transplant lymphoproliferative disorder before and after treatment and comparison with primary B cell central nervous system lymphoma. J Neurooncol 2015;125:297–305.
[6] Metser U, Lo G. FDG-PET/CT in abdominal post-transplant lymphoproliferative disease. Br J Radiol 2016;89:20150844.
[7] Lopez-Ben R, Smith JK, Kew CE 2nd, et al. Focal posttransplantation lymphoproliferative disorder at the renal allograft hilum. AJR Am J Roentgenol 2000;175:1417–22.
[8] Quinlan SC, Pfeiffer RM, Morton LM, et al. Risk factors for early-onset and late-onset post-transplant lymphoproliferative disorder in kidney recipients in the United States. Am J Hematol 2011;86:206–9.
[9] Pickhardt PJ, Siegel MJ. Posttransplantation lymphoproliferative disorder of the abdomen: CT evaluation in 51 patients. Radiology 1999; 213:73–8.
[10] Vrachliotis TG, Vaswani KK, Davies EA, et al. CT findings in posttransplantation lymphoproliferative disorder of renal transplants. AJR Am J Roentgenol 2000;175:183–8.
[11] Sharfuddin A. Imaging evaluation of kidney transplant recipients. Semin Nephrol 2011;31:259–71.
[12] Ali MG, Coakley FV, Hricak H, Bretan PN. Complex posttransplantation abnormalities of renal allografts: evaluation with MR imaging. Radiology 1999;211:95–100.
[13] Correas JM, Claudon M, Tranquart F, et al. The kidney: imaging with microbubble contrast agents. Ultrasound Q 2006;22:53–66.
[14] Noraini AR, Ferrara C, Ravelli E, et al. PET-CT as an effective imaging modality in the staging and follow-up of post-transplant lymphoproliferative disorder following solid organ. Singapore Med J 2009;50: 1189–95.
[15] Vegso G, Hajdu M, Sebestyen A. Lymphoproliferative disorders after solid organ transplantation-classification, incidence, risk factors, early detection and treatment options. Pathol Oncol Res 2011; 17:443–54.
[16] Trappe R, Hinrichs C, Appel U, et al. Treatment of PTLD with rituximab and CHOP reduces the risk of renal graft impairment after reduction of immunosuppression. Am J Transplant 2009;9:2331–7.
[17] Miyagi S, Sekiguchi S, Kawagishi N, et al. Rituximab therapy and reduction of immunosuppression to rescue graft function after renal posttransplantation lymphoproliferative disorder found by macrohematuria in a pancreas and kidney transplant recipient: a case report. Transplant Proc 2011;43:3299–301.
[18] Saadat A, Einollahi B, Ahmadzad-Asl MA, et al. Posttransplantation lymphoproliferative disorders in renal transplant recipients: report of over 20 years of experience. Transplant Proc 2007;39:1071–3.